Nanoscale Res Lett
DOI 10.1007/s11671-009-9384-9

NANO EXPRESS

A Study on Field Emission Characteristics of Planar Graphene Layers Obtained from a Highly Oriented Pyrolyzed Graphite Block

Seok Woo Lee · Seung S. Lee · Eui-Hyeok Yang

Received: 23 April 2009 / Accepted: 1 July 2009

Abstract This paper describes an experimental study on field emission characteristics of individual graphene layers for vacuum nanoelectronics. Graphene layers were prepared by mechanical exfoliation from a highly oriented pyrolyzed graphite block and placed on an insulating substrate, with the resulting field emission behavior investigated using a nanomanipulator operating inside a scanning electron microscope. A pair of tungsten tips controlled by the nanomanipulator enabled electric connection with the graphene layers without postfabrication. The maximum emitted current from the graphene layers was 170 nA and the turn-on voltage was 12.1 V.

Keywords Graphene · Field emission · Nanomanipulator · Nanoelectronics

Field emission is a quantum mechanical tunneling phenomenon in which electrons escape from a solid surface into vacuum, as explained theoretically by R. H. Fowler and L. Nordheim in 1928. Field emission is widely used in many kinds of vacuum electronic applications such as flat panel displays, microwave power tubes, electron sources, and electron-beam lithography. Over the past decade, research groups worldwide have shown that carbon nanotubes (CNTs) are excellent candidates for electron emission [1, 2]. CNTs possess advantages in aspect ratios, tip radius of curvature, chemical stability, and mechanical strength. However, issues related to the placement and throughput of CNT arrays has hampered the development of such arrays for commercial applications. Here, we use graphene for field emission.

Graphene is a two-dimensional honeycomb-structured single crystal showing ballistic transport, zero band gap, and electric spin transport characteristics [3–5]. In previous studies, graphene layers were randomly distributed on cathode electrodes for field emission display applications [6, 7]. However, further field emission studies are required using high-quality, planar graphene structure (e.g. obtained from a highly oriented pyrolyzed graphite (HOPG) block). In order to understand the fundamental behavior of graphene field emission and expand its application into vacuum nanoelectronics beyond the field emission display, the characterization and analysis of field emission from an individual graphene sheet is necessary.

In this paper, we suggest a new application for graphene in vacuum nanoelectronics. Figure 1 shows a conceptual schematic of a graphene-based triode device. Such a graphene triode structure can be used as a fundamental unit for vacuum nanoelectronics. The triode has an in-plane graphene tip (emitter) with the other in-plane electrodes used as source, drain, and gate on the substrate. Depending on the gate voltage applied, electrons are emitted from the graphene tip creating an electron current that can be modulated on and off. To realize this conceptual device, the field emission characteristics of graphene layers with different thicknesses need to be characterized.

To create the graphene layer for this experimental study, graphene sheets were prepared by mechanical exfoliation and placed on insulating SiO_2 substrate. Figure 2 shows the mechanical exfoliation process of graphene sheets on SiO_2. A thermo-curable elastomer, polydimethylsiloxane (PDMS,

S. W. Lee · S. S. Lee
Department of Mechanical Engineering, KAIST, Daejeon, Korea

E.-H. Yang (✉)
Department of Mechanical Engineering, Stevens Institute of Science and Technology, Hoboken, NJ, USA
e-mail: Eui-Hyeok.Yang@stevens.edu

Published online: 12 July 2009

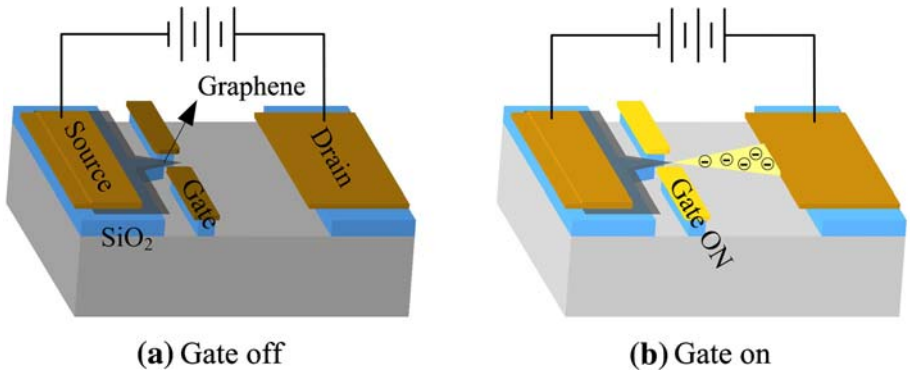

Fig. 1 Conceptual schematic view of a graphene-based triode as a fundamental unit for vacuum nanoelectronics. Depending on the gate voltage applied, electrons are emitted from the graphene tip creating an electron current that can be modulated on and off

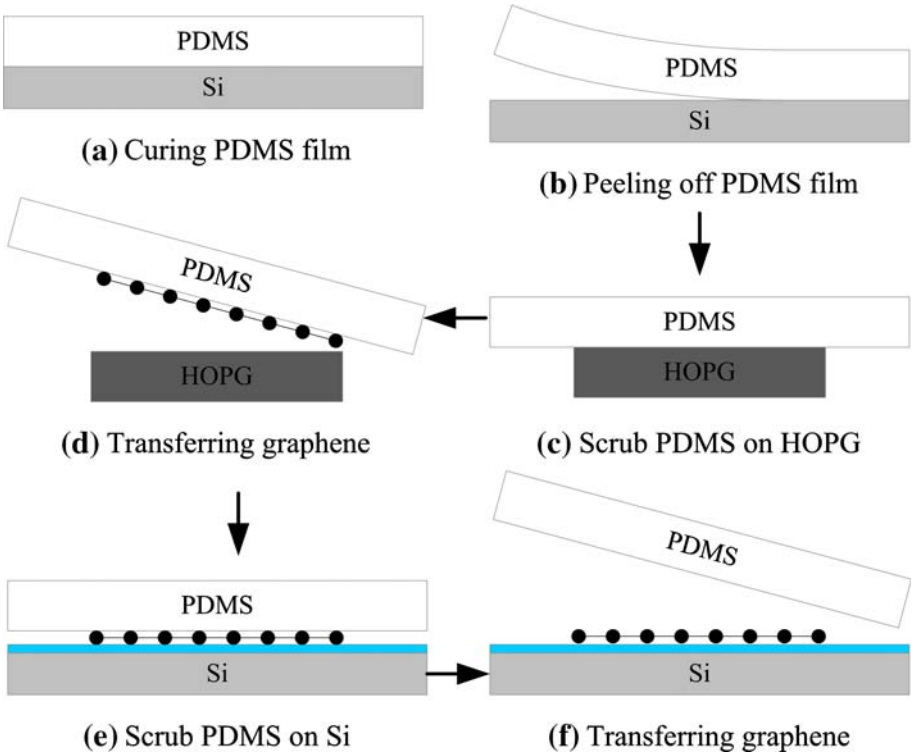

Fig. 2 Fabrication process of graphene sheets using a mechanical exfoliation method. The graphene sheets are transferred from HOPG block to SiO_2 layer

Sylgard 184, Dow Corning Co.) film was prepared using a standard recipe on an oxidized Si wafer (see Fig. 2a). The curing temperature and time were 65 °C and 4 h, respectively. After peeling the film from the wafer, its polished side was scrubbed on a highly oriented pyrolyzed graphite (HOPG) block (see Fig. 2b, c), and lifted off, transferring graphene layers to the PDMS (Fig. 2d). The exfoliated graphene layers were transferred onto SiO_2 thin film by scrubbing the PDMS film and subsequently detaching, leaving behind thin graphene layers (see Fig. 2e, f). In order to find and evaluate the graphene layers, the thickness of SiO_2 layer on Si was set to 300 nm considering optical interference [8].

A Zyvex Nanomanipulator operating inside a scanning electron microscope (SEM: XL-40 SEM, FEI Co.) was used to measure field emission from individual graphene sheets (Fig. 2). Figure 3 shows the schematic view of the experimental setup for measuring a field emission current from graphene sheets. In the SEM vacuum chamber, two tungsten tips were located on the graphene sample; one was contacted directly to the sample and grounded as a cathode, and the other was placed an arbitrary distance, d, apart from the edge of the sample as the anode. The tungsten tips were connected to a Keithley semiconductor measurement system via a feed-through in the vacuum chamber to apply and sense the electric signal for field emission. Figure 4a shows an optical image of the graphene sheets on SiO_2 layer. The thickness of the layer was optically measured on 300 nm thick SiO_2 layer by using the change of color due to optical interference and transparency [8]. The color change as the number of graphene layers varies is clearly distinguishable. In Fig. 4a, Cobalt blue, purple, and light

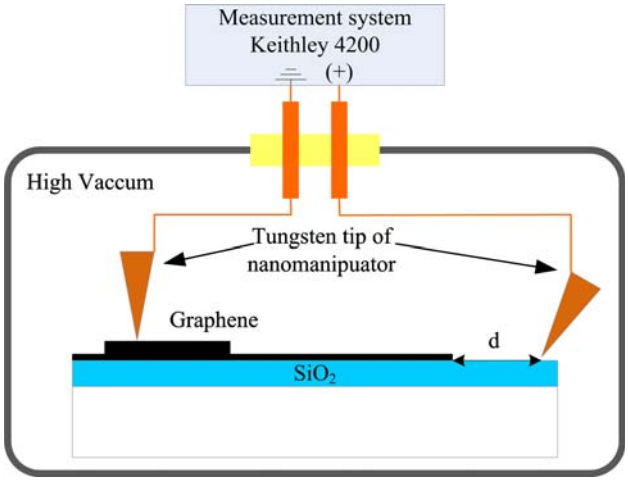

Fig. 3 Schematic view of the experimental setup using a nanomanipulator

purple stand for 8, 4 and 2 nm thicknesses, respectively. Figure 4b shows an SEM image of graphene sheets with a pair of tungsten tips controlled by the nanomanipulator.

After adjusting the position of the tips, a positive potential was applied to the second tip. The current was then measured during a voltage sweep. Figure 5a shows *I–E* curves of graphene for an arbitrary gap <1 μm. The graphene sheet started to emit electron current around 20 V and increased exponentially up to 170 nA following the behavior of the Fowler–Nordheim relationship. The field emission current fluctuated for applied voltages higher than 33 V. Figure 5b shows *F–N* curves obtained as a result of field emission from a graphene sheet. As shown in Fig. 5a, the emission current is increased exponentially, and the *F–N* curve shows linear relationship following the field emission behavior. The estimated turn-on voltages of the tested graphene sheet is 12.1 V, where the slope of *F–N* curve is changed and the linear region (red line) begins as shown in Fig. 5b. In order to estimate the field-enhancement factor, β, *F–N* parameters were evaluated by linear fit of the red line as shown in the equations [9, 10].

$$I(E) = A\frac{q}{8\pi^2\hbar\varphi}\frac{1}{\varphi}(\beta E)^2 \exp\left(-\frac{4}{3\hbar(\beta E)}\sqrt{2m\varphi^3}\right) \quad (1)$$

$$\left[\ln\frac{I}{E^2}\right] = -\frac{b}{\beta}\varphi^{\frac{3}{2}}\left[\frac{1}{E}\right] + \ln aA\beta^2 = -21.7\left[\frac{1}{E}\right] - 93.5 \quad (2)$$

$$b = 6.83 \times 10^3 \mathrm{V}^{-\frac{1}{2}}\mu m^{-1} \quad (3)$$

where I: current, E: electric field (V/d), β: field-enhancement factor, φ: work function, A: area, $\hbar$: reduced Planck constant, and m: electron mass. Assuming the work function of graphene is 5 eV and the gap between the graphene sheet and the nanomanipulator tip is 1 μm, the estimated field-enhancement factor, β, is 3519. It is found that the measured field-enhancement factor is comparable with previous results of graphene film prepared by electrophoresis [7], and the field emission efficiency of graphene is twice as high as other carbon nanomaterials such as CNT and diamond film [10, 11].

From the experimental results, it is found that one can further reduce the voltage for electron emission as the fabrication process is refined to create a fine emitter tip from graphene sheets. The field emission properties of graphene need further investigation in terms of the number of graphene layers and crystallographic arrangement of the carbon lattice. In the near future, a planar triode device will be studied for next generation vacuum nanoelectronics.

This field-emitting nanodevice based on the planar form of graphene potentially allows for top-down CMOS compatible process flows, an advantage for potential industrial fabrication of electronic devices. For applications where high field emission currents or low turn-on voltages are

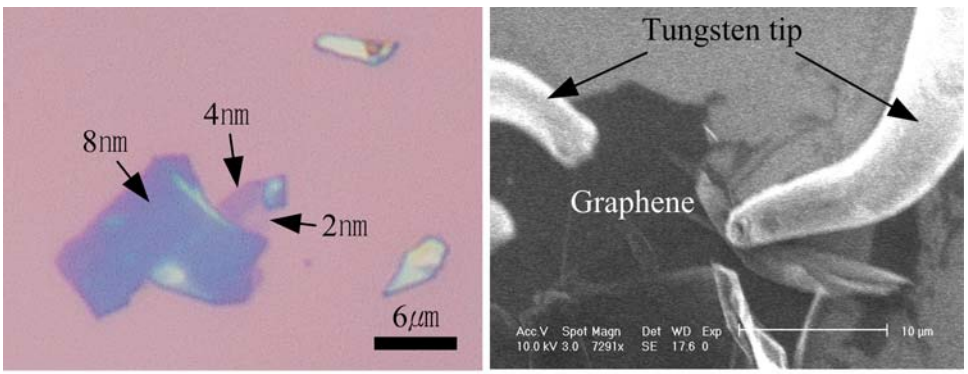

Fig. 4 Graphene sample **a** optical image of graphene sheets on SiO_2. The *color* of graphene sheets determines thickness of the graphene layer. *Scale bar*: 6 μm. **b** SEM image of a graphene sample with tungsten tips controlled by nanomanipulator

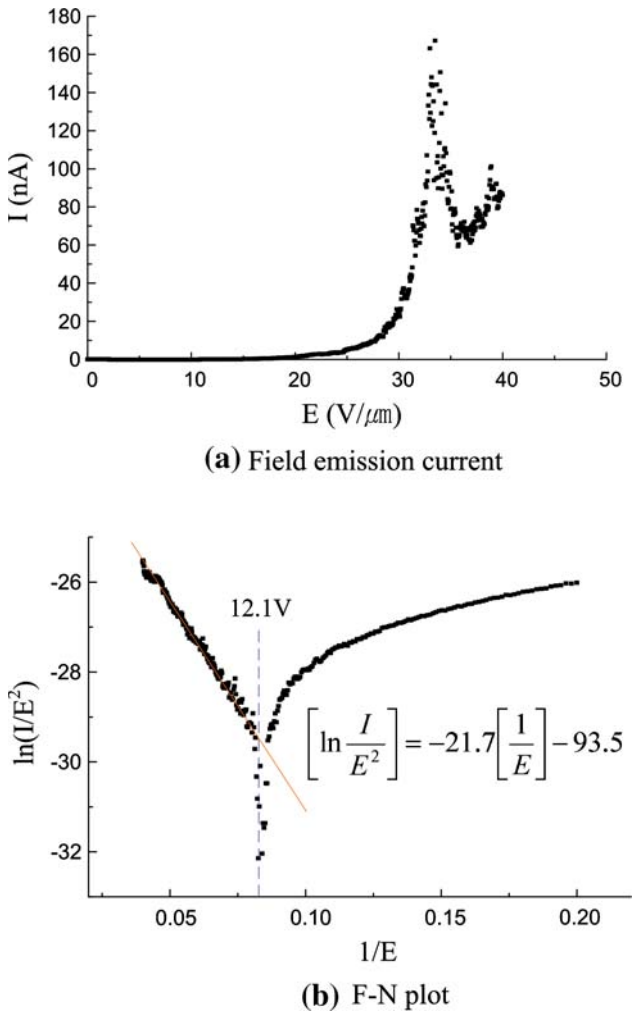

Fig. 5 **a** *I–E* plot for emission current. **b** *F–N* plot for emission current

required, nanodevices based on graphene would inherently provide the necessary alignment based on its crystallographic nature.

Acknowledgments This work has partially been supported by Exchange Student Program by Brain Korea 21, Award No KUK-F1-038-02 made by King Abdullah University of Science and Technology (KAUST) and National Science Foundation (Major Research Instrumentation Program, Award No. DMI-0619762).

References

1. W.A. de Heer, A. Chatelain, D. Uarte, Science **270**, 1179 (1995)
2. H.M. Manohara, M.J. Bronikowski, M. Hoenk, B.D. Hunt, P.H. Siegel, J. Vac. Sci. Technol. B **23**, 157 (2005)
3. A.K. Geim, K.S. Novoselov, Nat. Mater. **6**, 183 (2007)
4. K.S. Novoselov, A.K. Geim, S.V. Morozov, D. Jiang, Y. Zhang, S.V. Dubonos, I.V. Grigorieva, A.A. Firsov, Science **306**, 666 (2004)
5. N. Tombros, C. Jozsa, M. Popinciuc, H.T. Jonkman, B.J. van Wees, Nature **448**, 571 (2007)
6. J.J. Wang, M.Y. Zhu, R.A. Outlaw, X. Zhao, D.M. Manos, B.C. Holloway, V.P. Mammana, Appl. Phys. Lett. **85**, 1265 (2004)
7. Z.S. Wu, S. Pei, W. Ren, D. Tang, L. Gao, B. Liu, F. Li, C. Liu, H.-M. Cheng, Adv. Mater. **21**, 1756 (2009)
8. P. Blakea, E.W. Hill, H. Castro Neto, K.S. Novoselov, D. Jiang, R. Yang, T.J. Booth, A.K. Geim, Appl. Phys. Lett. **91**, 063124 (2007)
9. R.H. Fowler, L. Nordheim, Proc. R. Soc. (London) **A119**, 173 (1928)
10. X. Lu, Q. Yang, C. Xiao, A. Hirose, T. Tiedje, J. Phys. D Appl. Phys. **40**, 4010 (2007)
11. J.M. Bonard, R. Gaal, S. Garaj, L. Thien-Nga, L. Forro, K. Takahashi, F. Kokai, M. Yudasaka, S. Iijima, J. Appl. Phys. **91**, 10107 (2002)